Time-Base Nonlinearity Determination Using Iterated Sine-Fit Analysis

Gerard N. Stenbakken, *Member, IEEE,* and John P. Deyst, *Member, IEEE*

***Abstract*— A new method is presented to determine the time-base errors of sampling instruments. The method does not require a time-base error model and thus provides accurate estimates where model-based methods fail. Measurements of sinewaves at multiple phases and frequencies are used as test signals. A harmonic distortion model is used to account for amplitude nonlinearity of the sampling channel. Use of an independent method for estimating the channel noise and jitter allows an accurate estimate of the harmonic order. Methods are presented for separating the harmonics generated by the sampling channel from those generated by the time-base distortion. The use of an iterative sine-fit procedure gives accurate results in a short time. A new weighting procedure is described, which minimizes the error in the estimates. Guidelines are given for selecting good sets of test frequencies. Results are shown for both simulated and real data.**

***Index Terms*— Calibration, curve fitting, distortion, sampled data systems, timing, timing jitter.**

I. Introduction

DEVIATIONS in the sample intervals of sampling instruments cause nonlinear distortion of the sampled waveforms. If these deviations can be measured, corrections can be made to the sampled data, or the sampling intervals can be modified to correct them. The sample interval deviations have two components; a deterministic part called time-base distortion, and a random component called jitter.

A number of methods have been developed to measure time-base distortion. The "zero-crossing" methods [1]–[3] make use of waveforms of constant frequency, or carefully selected frequencies [4]. The resolution of these techniques is equal to the sine period, so they are limited by the bandwidth of the sampling channel. Early "sine-fit" methods assumed a pure sinewave input signal [5]; these methods do not easily handle harmonic distortion caused by the sampling channel of the instrument. An improved sine-fit method [6] is able to account for the harmonic distortion of the sampling channel. A time-base distortion determination method using the improved sine-fit method has been developed [7]. A phase demodulation technique called the "analytic signal" method [8] has also been described. Both the improved sine-fit and analytic signal methods use models for the time-base distortion, which prevent them from accurately estimating discontinuities in the time-base distortion, as shown in [9].

Manuscript received May 21, 1998; revised November 9, 1998.

The authors are with the Electricity Division, National Institute of Standards and Technology, Gaithersburg, MD 20899 USA (e-mail: stenbakken@eeel.nist.gov).

Publisher Item Identifier S 0018-9456(98)09758-7.

This paper describes a new method for determining time-base distortion, based on iterating the sine-fitting process. Because a time-base error model is not used, this method can accurately estimate discontinuities in the time-base. A harmonic model is used to account for the amplitude nonlinearity of the sampling channel, which allows determination of the distortion of the input signal or distortion caused by the channel. Use of the proper harmonic order is important for accurate time-base distortion estimation. If the model order is too low, some channel distortion will be attributed to the time-base error, and, if the model order is too high, some noise will be fit as channel distortion also increasing the time-base error. A method for determining the proper harmonic order is described that compares the sine-fit residuals to an independent assessment of the noise and jitter of the measurement process.

Time-base distortion estimates depend on the time derivative of the input signal. Where this derivative is small, the additive noise can either make the process unstable or make the estimates inaccurate. To overcome this problem, various weighting methods have been tried. Three are described here and one, a new weighting method, is shown by simulation to give the most accurate time-base distortion estimates. Since both nonlinear channel electronics and time-base distortions can generate harmonic distortions, the time-base estimation method must be able to distinguish the causes. Two methods are described for resolving this ambiguity; use of either two or more frequencies or a constant-waveshape constraint. Guidelines are given for good frequency pairs to use for good harmonic ambiguity resolution.

Since the iterative sine-fit procedure is a directed iterative process, it converges rapidly to an accurate result. Results for both simulated and real data are presented. This method is being used in an oscilloscope calibration software package under development at NIST [10].

II. Iterative Sine-Fit Method

A. Sampling Model

Fig. 1 shows the model used to describe the sampling channel [7]. The nonlinearity of the channel distorts the input signal $x(t)$ giving $s(t)$, which can be described by an h order harmonic distortion model [6] as

$$s(t) = A_0 + \sum_{l=1}^{h} A_l \sin(l\omega t + \phi_l) \tag{1}$$

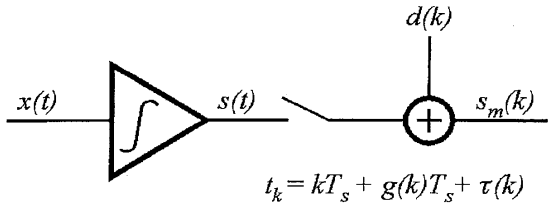

Fig. 1. Diagram of model used for sampling channel error sources.

where, in general, the $2h+1$ parameters in (1) are a function of the amplitude and frequency of the input signal. The kth sample time t_k is given by

$$t_k = kT_o + g(k)T_o + \tau(k) \tag{2}$$

where the three respective terms are the ideal sample time kT_s, the deterministic time-base distortion $g(k)$ times the sample period T_s, and the random jitter $\tau(k)$. The $\tau(k)$ are assumed to be independent and identically distributed (i.i.d.), with a zero mean and standard deviation of σ_τ. The sampled measurements are given by

$$s_m(k) = s(t_k) + d(k) \tag{3}$$

where $d(k)$ includes all the additive noise of the channel including the converter quantization noise and the input noise. The $d(k)$ are also assumed to be i.i.d. [and independent of $\tau(k)$] with a zero mean and standard deviation of σ_d. The sampled records of the measured signal will have N samples with k from 0 to $N-1$.

B. Motivation

Following [5] the sampled data values s_m can be fit with the harmonic distortion model (1) and the residuals of the fit attributed to the time-base distortion as

$$g(k) \approx \left.\frac{s_m(k) - s_e(t)}{T_s \dot{s}_e(t)}\right|_{t=kT_s} \tag{4}$$

where $s_e(t)$ is the $2h+1$ parameter fit (ω is the given input frequency and is not varied in the fitting process), and $\dot{s}_e(t)$ is the time derivative of $s_e(t)$.

This estimation for $g(k)$ suffers from several error sources. The most significant is that, if there is any time-base distortion, the samples are not taken at the ideal sample times of kT_s, and thus the parameters that give the estimate $s_e(t)$ are generally not correct. Also, the estimates for $g(k)$ are poor wherever $\dot{s}_e(t)$ is very small because of the noise in $s_m(k)$. The first problem is eliminated here with an iterative approach, where (4) gives the first order estimate of the time-base errors and then these new time values are used in (1) to fit the harmonic distortion model to unequally spaced samples. Then this new fit model is used in (4) and the process repeated until the changes in the fit residuals are minimized. This process estimates $N+2h+1$ parameters with only N data samples, so it is ill conditioned. However, if p records of the input signal ($p \geq 2$) are sampled with different phases of the same input frequency ω, then we have pN data samples and, since normally $N \gg h$, we have sufficient data samples to estimate the parameters. The phases can be chosen such that all sample points have at least one phase with a large value of $\dot{s}_e(t)$. As recommended in [5], the data from samples and phases with very small values of $\dot{s}_e(t)$ should not be included in the analysis. This elimination of some of the data samples is a form of weighting that will be described more fully in Section III.

However, the presence of time-base distortion can generate harmonics in the sampled data. The estimation process described so far cannot easily distinguish whether the time-base or the nonlinear input channel generated the harmonics. Two methods for removing this ambiguity are presented next. The multiple frequency method uses multiphase records at two or more frequencies. The constant-waveshape constraint method assumes that the distorted waveform shape does not change when the phase of the sampled signal is changed.

C. Multiple Frequency Method

If p_f phases at each of F frequencies of the input signal are sampled, then M records will be available, where $M = \sum_{f=1}^{F} p_f$. In general, the phases measured at each frequency need not be the same, nor must the number of phases measured at each frequency be the same. For $j = 1$ to M the M sampled waveforms are given by

$$s_m^j(k) = s^j(t_k) + d^j(k) \tag{5}$$

where

$$s^j(t_k) = A_0^j + \sum_{l=1}^{h} A_l^j \sin(l\omega^j t_k + \phi_l^j). \tag{6}$$

For the iterative sine-fit approach the initial time-base estimate is equally spaced samples $t_{k0} = kT_s$. The initial sine-fit estimates $s_e^j(t_k)$ are given by

$$s_{e0}^j(t_{k0}) = A_{00}^j + \sum_{l=1}^{h} A_{l0}^j \sin(l\omega^j t_{k0} + \phi_{l0}^j) \tag{7}$$

where the $2h+1$ parameters are the least squares solution from fitting (6) to $s_m^j(k)$. Equation (7) is iteration $i = 0$. Successive iterations are given by fitting

$$s_{ei}^j(t_{ki}) = A_{0i}^j + \sum_{l=1}^{h} A_{li}^j \sin(l\omega^j t_{ki} + \phi_{li}^j) \tag{8}$$

to $s_m^j(k)$, where

$$t_{k(i+1)} = t_{ki} + \frac{T_s}{w_T(k)} \sum_{j=1}^{M} w^j(k) g_i^j(k) \tag{9}$$

$$w_T(k) = \sum_{j=1}^{M} w^j(k) \tag{10}$$

and

$$g_i^j(k) = \left.\frac{s_m^j(k) - s_{ei}^j(t)}{T_s \dot{s}_{ei}^j(t)}\right|_{t=t_{ki}}. \tag{11}$$

The weighting factors $w^j(k)$ are discussed in Section III. At each iteration the fit error K_ε is calculated as

$$K_{\varepsilon i} = \left(\frac{1}{D_F} \sum_{j=1}^{M} \sum_{k=0}^{N-1} (s_m^j(k) - s_{ei}^j(t_{ki}))^2 \right)^{1/2} \quad (12)$$

where $D_F = MN - N - 2h - 1$ is the degrees of freedom. The iterations are stopped when the change in the fit error is below some tolerance δ_I, i.e., when $K_{\varepsilon(i-1)} - K_{\varepsilon i} \leq \delta_I$, or when the number of iterations has reached a limit n_I. The value of the fit error at convergence is called K_F, the final values for the sample time estimates from (9) are called $\hat{t}_k$, and the time-base distortion estimates are given by $\hat{g}(k) = (\hat{t}_k - kT_s)/T_s$.

D. Constant-Waveshape Constraint Method

Constant-waveshape constraint, the second method for removing the harmonic ambiguity, assumes that for different phases the waveform harmonic amplitudes and relative phases remain constant. This method of removing the harmonic ambiguity can be used together with the multiple frequency method. Thus, the description below assumes that the records are ordered into constant frequency groups and that this constraint is applied to the sampled waveforms in each frequency group. Since harmonic distortion is normally amplitude and frequency dependent, we assume that the p_f waveforms in each group have constant amplitude and frequency. Exactly how closely the amplitudes and frequencies must be maintained is dependent on how sensitive the harmonics are to these parameters. This will not be discussed here other than to point out that the signal frequencies are not a fitted parameter in this analysis and the error in the relative signal frequencies is assumed small compared to the jitter standard deviation relative to the record length.

The estimated harmonic amplitudes and phases for each group are averaged and the average amplitude and phase are used in the estimate for the time-base distortion. This is done by first decomposing each harmonic into a sinewave that crosses zero in phase with the fundamental plus a sinewave in quadrature. Thus, the fit estimates are given as

$$\begin{aligned} s_{e0}^j(t_{k0}) = {} & A_{00}^j + A_{10}^j \sin(\omega^j t_{k0} + \phi_{10}^j) \\ & + \sum_{l=2}^{h} \Big(B_{l0}^j \sin(l\omega^j t_{k0} + l\phi_{10}^j) \\ & + C_{l0}^j \cos(l\omega^j t_{k0} + l\phi_{10}^j) \Big) \end{aligned} \quad (13)$$

where

$$B_{l0}^j = A_{l0}^j \cos(\phi_{l0}^j - l\phi_{10}^j) \quad (14)$$

and

$$C_{l0}^j = A_{l0}^j \sin(\phi_{l0}^j - l\phi_{10}^j). \quad (15)$$

The B_{l0}^j and C_{l0}^j for each group are averaged. The constrained constant-waveshape fits $\overline{s}_{e0}^j$ are obtained by using these average values $\overline{B}_{l0}^j$ and $\overline{C}_{l0}^j$ in place of the individual harmonic amplitudes in (13) for all waveform estimates in each group. The constrained time-base distortion estimates at each iteration are given by

$$\overline{g}_i^j(k) = \left. \frac{s_m^j(k) - \overline{s}_{ei}^j(t)}{T_s \dot{\overline{s}}_{ei}^j(t)} \right|_{t=t_{ki}} \quad (16)$$

Note that in this implementation, the amplitudes of the fundamental in each group are not averaged. These values should be checked after convergence to verify that they are constant for all waveforms within each group.

III. Simulation Results

To apply these methods, some of the questions that need to be addressed are what harmonic order h and frequencies ω^j to use in (8) or (13), and what weighting factors $w^j(k)$ to use in (9). The appropriate harmonic order can be determined by looking at K_F as a function of h, $K_F(h)$. As h is increased $K_F(h)$ will decrease then level off at the proper h value. The expected value at which $K_F(h)$ should level off can be estimated from the standard deviation of repeat measurements of $s_m(k)$. Take M_R records of one phase of the input signal $s_m^j(k)$, $j = 1$ to M_R; then calculate the RMS of the standard deviations at each sample $\overline{\sigma}_{M_R}$ as

$$\overline{\sigma}_{M_R} = \left(\frac{1}{N} \sum_{k=0}^{N-1} \hat{\sigma}_{M_R}^2(k) \right)^{1/2} \quad (17)$$

where

$$\hat{\sigma}_{M_R}^2(k) = \frac{1}{M_R - 1} \sum_{j=1}^{M_R} (s_m^j(k) - \overline{s}_m(k))^2 \quad (18)$$

and

$$\overline{s}_m(k) = \frac{1}{M_R} \sum_{j-1}^{M_R} s_m^j(k). \quad (19)$$

The value at which $K_F(h)$ levels off should be close to $\overline{\sigma}_{M_R}$. As shown in [6], the estimated sample standard deviations $\hat{\sigma}_{M_R}(k)$ can be used to estimate the noise $\hat{\sigma}_d$ and jitter $\hat{\sigma}_\tau$ standard deviations of the measurement process by fitting $\hat{\sigma}_{M_R}^2(k)$ to the model $\hat{\sigma}_d^2 + \dot{s}_e(t)^2 \hat{\sigma}_\tau^2$.

A. Weighting

Three weighting methods were examined. In [5] unstable estimates from (11) are avoided by eliminating from analysis those values of k for which $s_e^j(\hat{t}_k)$ are within 15° of the peak, i.e., where $\dot{s}_e^j(t)$ approaches zero. That is

$$w_U^j(k) = \begin{cases} 1, & \text{if } |s_e^j(\hat{t}_k)| \leq \sin(75°) A_1^j \\ 0, & \text{if } |s_e^j(\hat{t}_k)| > \sin(75°) A_1^j. \end{cases} \quad (20)$$

This eliminates about one-sixth of the samples, and gives a uniform weight of one to the other samples. Weighting $w_U^j(k)$ is called uniform weighting.

The weighting method recommended in [6] is to weight each data sample proportionally to the inverse of its amplitude prediction uncertainty. This method, which uses estimates for

the noise $\hat{\sigma}_d(k)$ and jitter $\hat{\sigma}_\tau(k)$ standard deviations, and the signal derivative, weights each sample by

$$w_n^j(k) = \left(1 + \left(\frac{\dot{s}_e^j(t)\hat{\sigma}_\tau}{\hat{\sigma}_d}\right)^2\right)^{-(1/2)}\Bigg|_{t=\hat{t}_k}. \quad (21)$$

This weighting gives most weight to those samples where $\dot{s}_e^j(t)$ is near zero and least weight to those where $\dot{s}_e^j(t)$ is large. This will make some estimates from (11) unstable; to avoid that instability, the weighting given in [6] is multiplied by $w_U^j(k)$ and called noise weighting $w_{nU}^j(k)$.

The third weighting method considered is to weight each data sample proportionally to the inverse of its time prediction uncertainty. This weighting $w_\tau^j(k)$, called jitter weighting, is given by

$$w_\tau^j(k) = w_U^j(k)\left(1 + \left(\frac{\hat{\sigma}_d}{\dot{s}_e^j(t)\hat{\sigma}_\tau}\right)^2\right)^{-(1/2)}\Bigg|_{t=\hat{t}_k}. \quad (22)$$

Again, the term $w_U^j(k)$ is included to avoid instability. Note that if the channel errors are dominated by additive noise, this weighting is proportional to the derivative of the signal, whereas, if the jitter errors dominate, this weighting is close to the uniform weighting.

Simulations were performed to show the effects of the three weighting methods. The signal amplitude was one volt with no harmonic distortion ($h = 1$). Two frequencies and two phases were used, so M is 4. Sixty-four samples were made at a sample rate of 64 samples/s for each record, $T_s = 15.6$ ms. The two frequencies were 23 and 25 Hz and the two phases 0 and 90°. The time-base distortion was a ramp that varied from a distortion of −0.5 sample periods to 0.5 sample periods over approximately 22.4 samples, then repeated, giving 2.86 cycles of this distortion during the record. (Such a time-base distortion is not uncommon; see Fig. 4 as an example of real time-base distortion.) The phase of the distortion pattern was such that the first sample had zero time-base distortion. Thus, the distortion had three sharp jumps of −1 sample-periods. One thousand simulations were run using each weighting for two error cases. In case I the channel errors are dominated by a noise standard deviation σ_d of 10 mV, with a jitter standard deviation σ_τ of 0.001 sample periods or 15.6 μs. In case II the channel errors are dominated by the jitter standard deviation σ_τ of 0.01 sample periods or 156 μs, with a noise standard deviation σ_d of 1 mV. The RMS error in the time-base estimates T_{RMS} is calculated as

$$T_{\mathrm{RMS}} = \left(\frac{1}{MN}\sum_{j=1}^{M}\sum_{k=0}^{N-1}(t_k - \hat{t}_k)^2\right)^{1/2}. \quad (23)$$

Table I shows the mean RMS time-base estimate error and mean fit error K_F for the 1000 simulations. In both error cases the jitter weighting gives the lowest time-base estimate errors and lowest residual fit errors.

TABLE I
COMPARISON OF THE TIME-BASE ESTIMATE AND FIT ERRORS FOR DIFFERENT, NOISE, JITTER, AND WEIGHTING

σ_d	σ_τ	Weighting	T_{RMS}	K_F
10 mV	15.6 µs	Uniform w_U	62 µs	10.9 mV
		Noise w_{nU}	62 µs	11.0 mV
		Jitter w_τ	50 µs	10.0 mV
1 mV	156 µs	Uniform w_U	88 µs	15.7 mV
		Noise w_{nU}	96 µs	17.5 mV
		Jitter w_τ	88 µs	15.7 mV

TABLE II
COMPARISON OF THE TIME-BASE ESTIMATE AND FIT ERRORS FOR DIFFERENT HARMONIC MODELS

Harmonics	K_F	T_{RMS}
{1}	70.5 mV	450 µs
{1,2}	12.0 mV	64 µs
{1,2,3}	9.8 mV	52 µs
{1,2,3,4}	9.7 mV	53 µs

B. Model Order Selection

Simulations to show harmonic order selection used an input signal $s(t)$ with $h = 3$, $A_0 = 0$ V, $A_1 = 1$ V, $\phi_1 = 0°$, $A_2 = 100$ mV, $\phi_2 = 0°$, and $A_3 = 10$ mV, $\phi_3 = 30°$. Four records were used with the same sampling rate, record size, time-base distortion, signal frequencies, and phases as in the weighting simulations. The noise and jitter standard deviations are $\sigma_d = 10$ mV, and $\sigma_\tau = 15.6$ μs. Table II shows the mean T_{RMS} and K_F of 1000 simulations with different order harmonic models. Note that K_F decreases significantly from the first to second harmonic models and from the second to the third model, but does not change significantly from the third to the fourth model. This behavior correctly suggests that the proper model to select is $h = 3$. Note also that the change in the K_F tracks corresponding changes in the error in the time-base estimates, T_{RMS}. An independent estimate of the measurement channel errors was made from 100 repeat records of a signal with 23 Hz, 0° phase. Following [6], analysis of these records gives a repeat RMS standard deviation $\overline{\sigma}_{M_R}$ of 10.1 mV and noise and jitter standard deviations $\hat{\sigma}_d = 10$ mV and $\hat{\sigma}_\tau = 16$ μs. All three values are close to the expected values. The value at which K_F leveled off, 9.8 mV, is approximately the repeat RMS standard deviation, 10.1 mV.

C. Frequency Selection

The choice of appropriate input signal frequencies to give

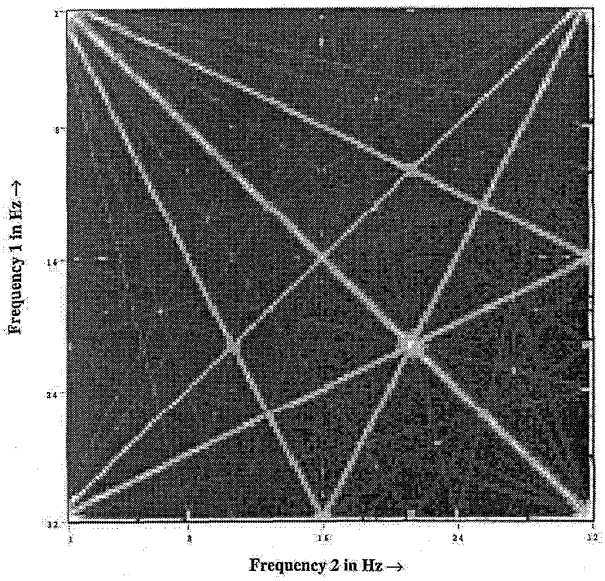

Fig. 2. Intensity plot of the $\log_{10}$ of the RMS time-base estimate errors, without constraint, axes show two frequencies in Hz.

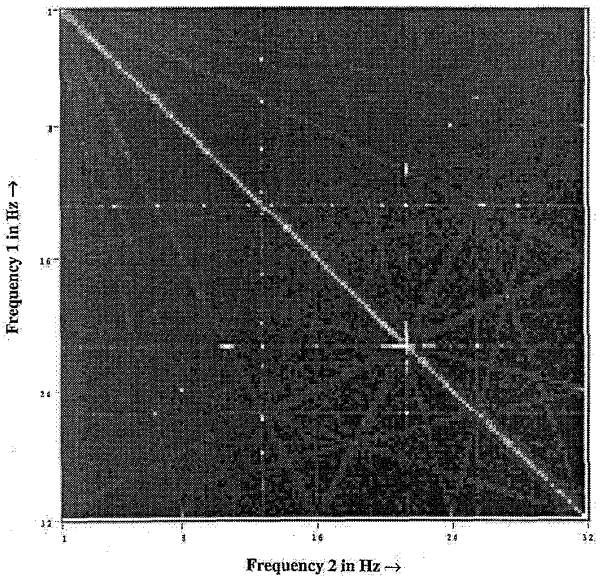

Fig. 3. Intensity plot of $\log_{10}$ of the RMS time-base estimate errors, with constant waveshape constraint, axes show two frequencies in Hz.

good discrimination between harmonics caused by the sampling channel and time-base distortion can be decided by looking at pairs of frequencies. For the three-harmonic signal model used in the above simulation, the RMS error in the time-base estimates, T_{RMS}, was simulated for many frequency pairs. The fit model used was the correct three-harmonic model. As above, four records were used with two phases, 0 and 90°, for each of the two frequencies. Fig. 2 shows an intensity plot of $\log_{10}(T_{\mathrm{RMS}})$, with a very small amount of noise and jitter added. This plot shows the matrix of frequency pairs obtained by varying each frequency from 1 Hz to the Nyquist frequency, $f_N = 32$ Hz. The intensities of the pixels are darker for frequency pairs that are good (lower T_{RMS}) and lighter for pairs not so good. The lighter diagonal lines delineate frequency pairs not to use. As the order of the fit model increases, more such lines appear on this kind of plot. The main diagonal shows the obvious poor choice of using pairs with the same frequency. Another line starting from the upper left below the main diagonal shows that one frequency f_1 should not be half the other frequency f_2 when the fit model contains second harmonics. Lines from the upper right shows that f_1 should not be the alias of f_2, $f_N - f_2$, nor twice the alias of f_2. A second but less bright set of lines show that the frequencies and aliases should not be related by a factor of 3 or a factor of 3 plus the sampling frequency f_s.

Fig. 3 is a similar plot with the constant-waveshape constraint applied. Even though there are only two phases in each group, this constraint has significantly reduced the error in the time-base estimates. While the diagonal lines have been reduced in intensity, several horizontal and vertical lines have appeared. These show that when the constant-waveshape constraint is applied, neither frequency should be one-third, one-fifth, or two-fifths the sampling frequency.

TABLE III
COMPARISON OF THE FIT ERRORS FOR DIFFERENT HARMONIC MODELS FOR THE DIGITIZER

Harmonics	K_F
{1}	5.16 mV
{1,2}	5.15 mV
{1,2,3}	4.83 mV
{1,2,3,4}	4.83 mV
{1,2,3,4,5}	4.83 mV

Some quality control parameters that are provided by this method will be briefly mentioned. For both these simulations the fit errors track the RMS time-base errors and thus can be used as a quality check on the proper selection of frequencies and phases. Also the lack of convergence within the iteration limit n_I, as happened for most of the pairs shown in light intensity on Figs. 2 and 3, indicate a poor data set.

IV. EXPERIMENTAL RESULTS

The iterative sine-fit method was applied to data taken on a commercial digitizer with a 50 GHz bandwidth. Analysis of repeat measurements of a 16 GHz input signal sampled at a rate of 512 samples per nanosecond, showed the random errors to be dominated by jitter. The jitter was measured to have a standard deviation of about 0.5 sample periods or 1 ps with no signal averaging. Twenty-four records with 4096 samples were analyzed to determine the time-base error. Each record is the average of ten repeat measurements taken at 512 samples per nanosecond. Twelve equally spaced phases were sampled at both 15.833 and 16 GHz. Table III shows the fit error K_F

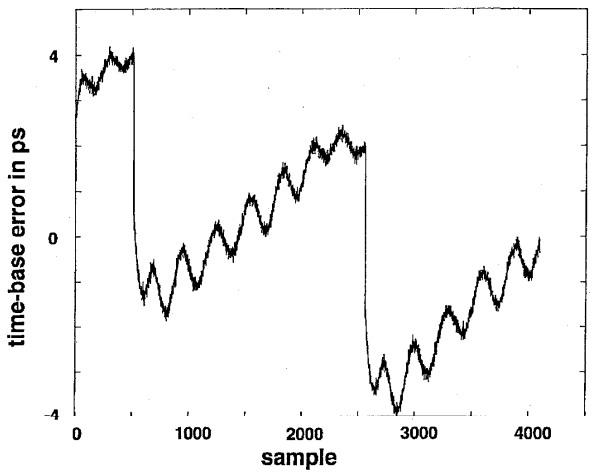

Fig. 4. Estimate of the time-base error of the HP 83480A digitizer.

as a function of the harmonics used in the fit model. Only the third harmonic appears to be significant from this analysis and it has a magnitude 39 dB below the fundamental, which was 220 mV.

Fig. 4 shows the time-base error measured for the digitizer. Note the pattern that repeats every 4 ns corresponds to the 250-MHz time-base clock. The damped sinewave pattern shows the time-base error from the clock interpolation circuitry.

V. Conclusions

A new method for determining the time-base distortion of sampling instruments has been described. It does not use a model for the time-base and provides accurate estimates even with discontinuities in the error. A problem with ambiguity of the source of harmonic distortion was described and two methods for resolving this ambiguity were presented. The use of records with two frequencies provides the greatest flexibility, and the constant-waveshape constraint provides a useful additional method. The problem of selecting the best pair of frequencies was described and relations between the two frequencies that should be avoided were presented. Three weighting methods were compared. The new jitter weighting method gives the lowest time-base estimate error. A method that uses the fit error to estimate the order of the harmonic model was described. The method was applied to simulated and real data.

Acknowledgment

The authors gratefully acknowledge the help provided by discussion of these methods with G. Vandersteen of the Vrije Universiteit Brussel, Department of Electrical Measurements, and the use of the digitizer data provided by him.

References

[1] W. R. Scott, Jr., "Error corrections for an automated time-domain network analyzer," *IEEE Trans. Instrum. Meas.*, vol. IM-35, pp. 300–303, Sept. 1986.
[2] A. M. Nicholson, "Broad-band microwave transmission characteristics from a single measurement of the transient response," *IEEE Trans. Instrum. Meas.*, vol. IM-17, pp. 395–402, Dec. 1968.
[3] W. L. Gans, "Calibration and error analysis of a picosecond pulse waveform measurement system at NBS," *Proc. IEEE*, vol. 74, pp. 86–90, Jan. 1986.
[4] J. B. Rettig and L. Dobos, "Picosecond time interval measurements," *IEEE Trans. Instrum. Meas.*, vol. 44, pp. 284–287, Apr. 1995.
[5] "IEEE Standard for Digitizing Wwaveform Recorders," IEEE Standard 1057-1994, Dec. 1994.
[6] R. Pintelon and J. Schoukens, "An improved sine wave fitting procedure for characterizing data acquisition channels," *IEEE Trans. Instrum. Meas.*, vol. 45, pp. 588–593, Apr. 1996.
[7] J. Schoukens, R. Pintelon, and G. Vandersteen, "A sinewave fitting procedure for characterizing data acquisition channels in the presence of time base distortion and time jitter," *IEEE Trans. Instrum. Meas.*, vol. 46, pp. 1005–1010, Aug. 1997.
[8] J. Verspecht, "Accurate spectral estimation based on measurements with a distorted-timebase digitizer," *IEEE Trans. Instrum. Meas.*, vol. 43, pp. 210–215, Apr. 1994.
[9] G. N. Stenbakken and J. P. Deyst, "Comparison of time base nonlinearity measurement techniques" *IEEE Trans. Instrum. Meas.*, vol. 47, pp. 34–39, Feb. 1998.
[10] J. P. Deyst *et al.*, "A fast pulse oscilloscope calibration system," this issue, pp. 1037–1041.

Gerard N. Stenbakken (M'71), for a photograph and biography, see this issue, p. 1041.

John. P. Deyst (M'90), for a photograph and biography, see this issue, p. 1036.